

# *Ab initio* evaluation of local effective interactions in $\alpha'NaV_2O_5$

Nicolas Suaud and Marie-Bernadette Lepetit

*Laboratoire de Chimie Quantique et Physique Moléculaire,  
Unité Mixte de Recherche 5626 du CNRS,  
118 route de Narbonne, F-31062 Toulouse, France*

(November 21, 2018)

We will present the numerical evaluation of the hopping and magnetic exchange integrals for a nearest-neighbor  $t - J$  model of the quarter-filled  $\alpha'NaV_2O_5$  compound. The effective integrals are obtained from valence-spectroscopy *ab initio* calculations of embedded crystal fragments (two  $VO_5$  pyramids in the different geometries corresponding to the desired parameters). We are using a large configurations interaction (CI) method, where the CI space is specifically optimized to obtain accurate energy differences. We show that the  $\alpha'NaV_2O_5$  system can be seen as a two-dimensional asymmetric triangular Heisenberg lattice where the effective sites represent delocalized  $V - O - V$  rung entities supporting the magnetic electrons.

## I. INTRODUCTION

Spin-Peierls (SP) transitions have been long known in organic compounds<sup>1</sup> but the observation, in 1993, of a SP transition in the inorganic  $CuGeO_3$ <sup>2</sup> ( $T_{SP} = 14K$ ) renewed the interest of the physical community for this phenomenon. In 1996 the  $\alpha'NaV_2O_5$ <sup>3</sup> inorganic system was found to present a second order SP transition<sup>4</sup> at  $T_{SP} = 34K$ , the highest  $T_{SP}$  temperature so far known. Indeed a rapid drop of the magnetic susceptibility, the opening of a spin gap<sup>5</sup> ( $\Delta = 9.8meV$ ) as well as the magneto-distortion of the lattice was observed in this compound. This compound has attracted special attention since, in addition of its very high  $T_{SP}$ , the value of the  $\frac{2\Delta}{k_B T_{SP}} = 6.44$  ratio does not agree with the BCS theory predicted value of 3.53, the  $T_{SP}$  dependence with the magnetic field is much weaker<sup>6</sup> than the theoretical predictions<sup>7</sup> and the temperature dependence of the thermal conductivity is much larger than in  $CuGeO_3$ <sup>8</sup>.

The crystal is formed by layers of  $VO_5$  square-pyramids stacked along

the  $c$  axis. The oxygen atoms of the pyramid basis form a quasi-square planar lattice along the  $a$  and  $b$  directions. The pyramids are alternatively pointing on top or below these planes. Periodical vacancies of the  $VO$  top of the pyramids are replaced by  $Na^+$  ions forming chains parallel to the  $b$  axis (see fig. 1).

For a long time, the high temperature crystal structure was assumed to be non-centrosymmetric (in  $P2_1mn$  group)<sup>9</sup>, and consequently the electronic structure was assumed to be an alternation of half filled  $V^{4+}$  magnetic chains and of non-magnetic  $V^{5+}$  chains along the  $b$  axis. The system was then supposed to be constituted of isolated Heisenberg chains and the SP transition was naturally understood in this description by the one-dimensional dimerization of the  $V^{4+}$  magnetic chains.

However the existence of a pseudo-inversion center in this compound led a couple of groups<sup>10</sup> to re-investigate the crystallographical data using more recent experimental methods. They found that  $\alpha'NaV_2O_5$  was centrosymmetric (in the  $Pm\bar{m}n$  space group) destroying the grounding for the assumed differentiation between  $V^{4+}$  and  $V^{5+}$  chains.  $\alpha'NaV_2O_5$  should then be seen as a quarter-filled system.

It is widely accepted, after Galy<sup>11</sup>, that the magnetic interactions take only place within the layers, and thus the pertinent model for  $\alpha'NaV_2O_5$  is a quarter-filled  $t - J$  model Hamiltonian in the  $(a, b)$  plane, based on the  $V$  magnetic  $3d$  orbitals, where the interactions are limited to the nearest neighbors (NN) magnetic sites.

$$H = \sum_{\langle i,j \rangle} t_{ij} \sum_{\sigma} (c_{i\sigma}^{\dagger} c_{j\sigma} + c_{j\sigma}^{\dagger} c_{i\sigma}) - \sum_{\langle i,j \rangle} J_{ij} \left( \vec{S}_i \cdot \vec{S}_j - \frac{1}{4} n_i n_j \right) \quad (1)$$

where the sum over  $\langle i, j \rangle$  runs over NN magnetic sites,  $\vec{S}_i$  is the local spin operator on site  $i$ ,  $c_{i\sigma}^{\dagger}$  (resp.  $c_{i\sigma}$ ) are the usual creation (resp. annihilation) operators of an electron of spin  $\sigma$  on site  $i$ ,  $n_i$  is the number operator on site  $i$ ,  $J_{ij}$  is the magnetic exchange integral and  $t_{ij}$  the hopping integral of a magnetic electron between sites  $i$  and  $j$ .

In the present system one has three different types of NN interactions (see fig. 2) : the interactions along the ladders (in the  $b$  direction) denoted as  $t_{\parallel}$  and  $J_{\parallel}$ , the interactions along ladders rungs denoted as  $t_{\perp}$  and  $J_{\perp}$  (in the  $a$  direction) and the interactions between the ladders denoted as  $t'$  and  $J'$ . According to the order of magnitude of these parameters, the system electronic structure can be very different, going from a one dimensional behavior with essentially non interacting two-legs ladders ( $|t'|, |J'| \ll 1$ ), or zig-zag frustrated ladders ( $|t_{\perp}|, |J_{\perp}| \ll$

1) to a two-dimensional system. It is therefore of crucial importance to have a reliable evaluation of the relative amplitude of the different parameters.

The aim of this work is to evaluate, using *ab initio* quantum chemical methods, the effective hopping and exchange integrals between NN vanadium atoms.

## II. METHOD

The exchange and hopping effective integrals are essentially local parameters, therefore they can be accurately evaluated using fragment spectroscopy, provided that (i) the fragment includes all the crystal short range effects, that is the local environment of the magnetic atoms, and (ii) the crystal long range effects are treated through an appropriate bath.

We performed excitation energies calculations on bi-pyramidal fragments (including the two NN magnetic atoms as well as all their surrounding oxygens) in a bath reproducing the main effects of the rest of the crystal (Madelung potential and exclusion effects). The fragments used for the  $t_{\parallel}$  (resp.  $J_{\parallel}$ ) and  $t_{\perp}$  (resp.  $J_{\perp}$ ) calculations are built from two  $VO_5$  pyramids sharing a corner (see fig. 3 a and b) while the fragment used for the  $t'$  (resp.  $J'$ ) calculations is constituted of two  $VO_5$  pyramids sharing an edge (see fig. 3 c). Two sets of calculations are performed for each fragment. The first one involving two unpaired electrons in the two  $VO_5$  pyramids allows us to obtain the effective exchange parameters (including all direct and super-exchange processes) from the singlet-triplet first excitation energy.

$$J = E_S - E_T \quad (2)$$

The second set of calculations, involving only one unpaired magnetic electron in the two  $VO_5$  pyramids, allows us to obtain the effective hopping parameters from the first doublet-doublet excitation energy.

$$t = \frac{E_{D_+} - E_{D_-}}{2} \quad (3)$$

where the  $D_+$  (resp.  $D_-$ ) doublet is of the same symmetry than the  $3d_1 + 3d_2$  (resp.  $3d_1 - 3d_2$ ) delocalized orbital on the two magnetic centers. One notes that according to the relative energies of the  $D_+$  and  $D_-$  states, the sign of the hopping integral can change.

### A. Modeling the rest of the crystal

As state above a correct fragment calculation should take into account the main effects of the rest of the crystal. In our ionic, strongly correlated system these effects are limited to the short range Pauli exclusion effects and the long range Madelung potential.

First, the Madelung potential is reproduced by a set of positive and negative charges corresponding to the cations and anions. We used a cutoff threshold associated with a  $13\text{\AA}$  radius sphere, centered on the bi-pyramid fragment. The border of the sphere is designed so that to preserve  $VO_5$  pyramids, the chemical meaningful entities. Border charges are adapted by an Evjen procedure.

The  $\alpha'NaV_2O_5$  system presents 4 different types of atoms : the fully ionized sodium cations, the mixed valence vanadium atoms and two types of oxygen atoms, the in-plane oxygens and the apical oxygens. These two types of oxygen play a very different role in the chemistry of the compound. Indeed, ab-initio calculations on the bi-pyramidal systems, both at the Hartree-Fock (HF) and correlated level, as well HF calculations on the whole crystal give the same result, the apical oxygen is bonded to the vanadium atom by a slightly polarized double bond. The Mülliken population analysis are similar in all calculations with a charge close to  $-2\bar{e}$  for the in-plane oxygens while the apical ones present only a small charge of about  $-0.5\bar{e}$ . In fact the  $VO_5$  pyramids should not be seen as such, but rather as  $(V = O)^{2+}$  or  $^{3+}$  molecules on an oxygen double-anions square lattice. This picture is confirmed by Raman experiments<sup>12</sup>. Indeed, two distinct bands are observed, one for the stretch of the vanadium/apical-oxygen bond located at  $970\text{ cm}^{-1}$ , the other for the group of vibrations of the vanadium against the oxygen plane which is located in the  $400\text{-}480\text{ cm}^{-1}$  range.

The embedding charges are then taken as follow :

- the sodium atoms are represented by  $+1.0\bar{e}$  charges,
- the oxygen atoms of the quasi-square lattice forming the basis of the pyramids are represented by  $-2.0\bar{e}$  charges,
- the apical oxygens are represented by  $-0.5\bar{e}$  charges
- and the vanadium atoms are represented by their average valence of  $+3.0\bar{e}$ .

Second, the exclusion effects are taken into account through total charges pseudo-potentials. The embedded fragments are highly nega-

tively charged ( $-8\bar{e}$  or  $-9\bar{e}$ ) and their electrons would like to expand out of the fragments volume, thus the contention effect of the rest of the crystal needs to be modeled by an exclusion potential. The negative charge of the oxygen anions, even modeled as point charges, is sufficient to insure the exclusion effect on the fragment electrons ; however the positive charge of the cations attracts the fragment electrons and it is necessary to explicitly treat the exclusion. This is done by modeling the cations with total-ions pseudo-potentials<sup>13</sup>, using the Durand and Barthelat large core effective potentials<sup>14</sup>, instead of only point charges.

The good behavior of the above embedding has been checked against HF crystal calculations. Figure 4 shows the Projected Density of States (PDOSS) on the magnetic orbitals of the vanadium atoms (1) and on the  $p$  orbital of the bridging oxygen of the rungs (2). The PDOSS is compared with its equivalent in the cluster calculations, the square of the cluster orbitals projection onto the atomic orbitals, plotted as a function of the cluster orbital energies. One can see that while the above embedding yields a favorable comparison of the cluster orbitals with the crystal PDOSS, the embedding defined with only one kind of oxygen atoms and the formal charges ( $O^{-2}$ ,  $V^{+4.5}$ ,  $Na^{+}$ ) do not properly place the vanadium  $d$  orbitals, in particular the gap at the Fermi level is overestimated. In order to emphasize the importance of a proper embedding, the isolated cluster orbitals are also reported. The result goes without comment.

## B. Computing accurate excitation energies

*Ab initio* quantum chemical methods are powerful tools to obtain reliable excitation energies as well as good representation of the associated ground or excited states wave functions. As will be seen later a precise analysis of the wave function informations allows a deep understanding of the different mechanisms involved in the effective exchange and hopping processes.

Let us first consider the physics of the excitations we are trying to compute. One sees easily that the fragment orbitals can be divided into three subsets according to their role in the many-body wave functions of the two states we are looking for.

**The occupied orbitals** are the orbitals that always remain doubly-occupied in the many-body states.

**The active orbitals** are the ones which occupation number can

change in the different Slater determinants participating to the many-body states. In our case these orbitals are not only the two  $3d$  magnetic orbitals (from now on we will refer to them as  $d_1$  and  $d_2$  according to the  $V$  atom to which they belong) located on the two vanadium atoms but also the  $2p$  orbitals (we will refer to them as  $p$ ) of the bridging oxygen atom(s) that can participate to the effective exchange through super-exchange mechanism and to the hopping process by a through bridge delocalization of the hole. Symmetry considerations reduce the number of these bridging orbitals to two  $2p$  orbitals (one per irrep. involved). One should note that these active orbitals correspond to the valence orbitals that would support a three-bands Hubbard representation of the system — where both the  $V$  and the  $O$  atoms of the pyramids bases are considered.

**The virtual orbitals** are the orbitals that always remain empty in the many-body states.

A good “zeroth-order” description of the sought states will then be provided by the eigensolutions of the exact Hamiltonian in the Complete Active Space (CAS) ; the CAS is defined as all possible configurations built from the occupation rules given above. In fact we simultaneously optimize the orbitals and the wave function coefficients in a Complete Active Space Self Consistent Field (CASSCF) procedure<sup>15</sup>. At this level of calculation, the polarization and correlation effects within the active space (static polarization and correlation) are variationally taken into account, while the other electrons are described within a mean field approximation. In the  $J$  calculations, six electrons — the two unpaired electrons plus the four electrons originating from the bridging  $p$  orbitals of the central oxygen(s) — are distributed in all possible manners into the four active orbitals. In  $t$  calculations, only five electrons are distributed into the four active orbitals.

“Dynamical” polarization and correlation effects coming from excitations out of the active shell (originating from the occupied orbitals or ending in the virtual ones) are however crucial in order to obtain reliable results for excitation energies. The “dynamical” polarization effects come from the single-excitations on the CASSCF wave function, while the dominant contributions to “dynamical” correlation effects come from the double-excitations on the CASSCF wave function. We will take these effects into account in a two steps procedure.

a) A self-consistent procedure is performed. It involves the diagonalization of the CAS + all single excitations space as well as a new orbitals optimization at this level. This is the so-called Iterative Difference Dedicated Configuration Interaction level 1 method (IDDCI1)<sup>16</sup>.

b) In a second step the double excitations on the CAS wave-function that participate to the energy difference (at the  $2^{nd}$  order of perturbation) are added to the CI space, which is diagonalized. This is the Difference Dedicated Configuration Interaction level 2 (DDCI2)<sup>17</sup>.

The above method is powerful and reliable. It has been used with great success in a slightly different version (DDCI3) for the determination of the  $t - J$  model parameters, for instance, on copper-oxides<sup>18</sup> or ladder compounds such as  $SrCu_2O_3$ <sup>19</sup>. The main differences between the procedure used in the present work and the works cited above are i) the optimization of the orbitals at the CAS + single excitations level (IDDCI1) instead of only at the CASSCF level ii) the inclusion of the dynamical polarization and correlation of the bridging oxygen  $p$  orbitals is done in a slightly different way. We choose to include the active orbital(s) of the bridge in the CAS so that the dynamical polarization effects are taken into account in the DDCI1 space and the dynamical correlation effects are taken into account in the DDCI2 space. De Graaf *et al*<sup>19</sup> as well as Calzado *et al*<sup>18</sup> made the choice of a smaller CAS including only the two magnetic  $d$  orbitals and to extend the diagonalization to the 2-holes 1-particle and 2-particles 1-hole CI space (DDCI3) in order to describe the same physics. The main advantages of our choice are the following

- The optimization of the orbitals at a level including the dynamical polarization effects.
- An equal treatment of the magnetic  $d$  orbitals and the active  $p$  orbitals of the bridge. This point can be important in the cases where the through bridge processes are large.
- A much smaller size of the largest CI space to diagonalize. For instance in the calculation of the  $J_{\perp}$  effective integral our choice yields a CI space of 592,000 determinants while the DDCI3 space with the small CAS would give a CI of 2,783,000 determinants.

In order to analyze the relative contributions of dynamical polarization and correlation we performed an additional Configuration Interaction, namely the diagonalization of the CAS but defined on the set of orbitals optimized within the IDDCI1 procedure (CASCI).

### C. Computational details

All cluster calculations are performed using the Barandiaran basis sets<sup>20</sup> with the recommended contraction:  $3s3p4d$  for  $V$  atoms and

$2s4p1d$  for  $O$  atoms. The effects of the inner electrons are modeled by core pseudo-potentials<sup>20</sup>,  $[1s^22s^22p^63s^2]$  for  $V$  atoms and  $[1s^2]$  for  $O$  atoms.

The crystal HF calculations were performed using the CRYSTAL98 package<sup>21</sup>. In order to be able to perform the infinite crystal calculation it has been necessary to reduce the basis set compared to the cluster calculations. We therefore used a basis set<sup>22</sup> of quality single-zeta for the core electrons, while the valence electrons were described using a double-zeta, plus one polarization function for the oxygen and two polarization functions for the vanadium.

### III. RESULTS AND DISCUSSION

The computed hopping and exchange integrals are summarized in table I.

The differences observed between the CASCI and the IDDCI1 results point out the crucial importance of the inclusion of dynamical *polarization* effects in order to obtain reliable results for effective exchange and hopping processes. In comparison the dynamical correlation effects are of much lesser importance since they modify the integrals amplitude by a factor of only 10% to 20%.

The computed wave functions are reported in the Appendix. Their analysis shows the strong contributions of  $O^-$  configurations on the bridging oxygen in the  $\perp$  geometries and moderate ones in the  $\parallel$  geometries. These configurations are negligible in the prime geometry, where their weight is smaller than 1%. This is easily understood by the quasi-orthogonal character of the angles between the Vanadium atoms and the two bridging Oxygens, this quasi-orthogonality strongly hinders the overlap between the V magnetic orbitals and the  $p$  orbitals of the bridging oxygens. Finally it results in the ferromagnetic character of  $J'$  and the weakness of the  $t'$  hopping integral.

In the rung or orthogonal geometry, the contribution of the  $O^-$  configurations is particularly large with weights of 15% in the triplet state, 25% in the singlet state and weights as large as 49% ( $D_-$ ) and 53% ( $D_+$ ) in the two doublet states. This tremendous delocalization of the magnetic electron on the  $p$  orbital of the bridging oxygen is responsible for the accordingly large hopping integral  $t_\perp$ , indeed the direct (by opposition to the through bridge) hopping mechanism contributes only by a few  $meV$  to the total amplitude. Similarly the strong  $O^-$  contributions in the singlet and the triplet states induce a large super-exchange

mechanism responsible for the strong anti-ferromagnetic character of  $J_{\perp}$ . Different reasons can be pleaded to explain these very large delocalization of the magnetic electrons on the bridging oxygen. The most important is the relative positions of the pyramids with respect to the bridging O atoms. The vanadium magnetic  $3d$  orbitals are orthogonal to the  $V = O$  bonds and the angle of the  $V = O$  bond to the oxygen plane is closed, the corresponding tilting of the vanadium magnetic orbitals toward the oxygen plane enhances considerably the overlap between these orbitals and the  $p$  orbitals of the bridging oxygen. Another important factor is the short distance ( $1.83\text{\AA}$ ) between the vanadium atoms and the bridging oxygen in this geometry.

The  $\parallel$  geometry is slightly different since two  $p$  orbitals (of different symmetries) of the bridging oxygen are involved in the through bridge processes. Their consolidated weights in the doublet states are 20% in  $D_-$  and 26% in  $D_+$  and they result in a moderate enhancement of  $t_{\parallel}$ . In the singlet and triplet states however, the  $O^-$  configurations do not contribute in a significant way to the wave functions since their consolidated weight is smaller than 1%. The result is a very weak superexchange mechanism resulting in a slightly anti-ferromagnetic effective exchange integral ( $J_{\parallel} \simeq J_{\perp}/60$ ).

The dominant interactions are by far those taking place on the ladder rungs ( $t_{\perp} = -538.2\text{meV}$  and  $J_{\perp} = -293.5\text{meV}$ ), thus they should determinate the main representation of the electronic structure. Two different descriptions can be proposed depending which of the exchange or the delocalization processes shall dominate. Either two electrons are paired in a singlet, one rung out of two (favored by the large value of  $J_{\perp}$ ), or an unpaired electron is delocalized on each rung (favored by the large hopping integral  $t_{\perp}$ ). A simple energetic calculation shows however that the second solution is much more favorable — with  $E_2/N_{rungs} = t_{\perp} = -538.2\text{meV}$  — than the first one —  $E_1/N_{rungs} = 1/2J_{\perp} = -147\text{meV}$ . On the basis of such a representation, the  $\alpha'NaV_2O_5$  system can be seen as a two dimensional triangular Heisenberg system (see fig. 5) where the effective magnetic sites are delocalized on the  $V - O - V$  rungs, in agreement with the representation suggested by Horsch and Mack<sup>23</sup>. A wave-functions analysis of the two many-body states involved in the  $t_{\perp}$  calculations confirm this result since the determinants involving an unpaired electron on the bridging oxygen are as probable as the determinants where the magnetic electron is located on the vanadiums. Indeed their relative weights are 1.00 in the  $D_-$  and 1.21 in the  $D_+$ . The exchange integrals between these effective sites are then anti-ferromagnetic in the  $b$  direction,  $J_{\parallel}^{eff} = J_{\parallel}/2$ , and ferromagnetic between the effective chains (representing the ladders),  $J'_{eff} = J'/4$ .

## IV. THE EXTENDED HUBBARD MODEL

### A. Coherence of the $t - J$ parameters

One of the first reflexes in front of quantitative evaluations of effective integrals in a  $t - J$  model is to check the following relation

$$\frac{J_{\perp}}{J_{\parallel}} = \left( \frac{t_{\perp}}{t_{\parallel}} \right)^2 \quad (4)$$

A quick calculation, using table I results, shows that the above relation is far from being verified in our case. Why?

Equation 4 comes from a perturbative evaluation,  $J = -4t^2/U_d$ , of the exchange integral from an underlying Hubbard or extended Hubbard model, supposed to be the exact representation. We saw in the previous section that the contributions of the  $O^-$  configurations are tremendously large in the rung geometry, a Hubbard model based only on the magnetic  $d$  orbitals of the vanadium atoms is therefore not realistic and any representation pretending to be *the reference* should include the  $p$  orbital of the bridging oxygen (at least in the rung geometry).

We will use the following notations: subscripts  $p$  and  $d$  respectively refer to the  $p$  orbital of the bridging oxygen and the magnetic  $d$  orbital of the vanadium.  $\delta = \epsilon_d - \epsilon_p$  is the orbital energy difference.  $U_p$  and  $U_d$  are the on-site repulsion energies.  $V_{pd}$  is the vanadium-oxygen nearest neighbor coulombic repulsion. The hopping integrals require a little more care since they can be encountered in different situations according to the number and nature of the surrounding electrons:

$$\begin{aligned} \langle \bar{p} | H | \bar{d} \rangle &= \langle \bar{p} | h | \bar{d} \rangle \\ \langle d\bar{p} | H | d\bar{d} \rangle &= \langle \bar{p} | h | \bar{d} \rangle + \langle d\bar{p} | V | d\bar{d} \rangle \\ \langle p\bar{p} | H | p\bar{d} \rangle &= \langle \bar{p} | h | \bar{d} \rangle + \langle p\bar{p} | V | p\bar{d} \rangle \\ \langle dp\bar{p} | H | dp\bar{d} \rangle &= \langle \bar{p} | h | \bar{d} \rangle + \langle p\bar{p} | V | p\bar{d} \rangle + \langle d\bar{p} | V | d\bar{d} \rangle \end{aligned}$$

where  $h$  refers to the mono-electronic part (kinetic and nuclear attraction) of the Hamiltonian and  $V = 1/r_{12}$  is the bi-electronic repulsion. The  $p$  and  $d$  orbitals being localized on nearest neighbor atoms, the  $\langle p\bar{p} | V | p\bar{d} \rangle$  and  $\langle d\bar{p} | V | d\bar{d} \rangle$  bi-electronic integrals are a priori of the same order of magnitude as the mono-electronic part of the hopping  $\langle \bar{p} | h | \bar{d} \rangle$ ; thus one should consider 4 different types of hopping integrals according to the number and the nature of the spectator electrons on the bond where the hopping takes place. Let us define

$$\begin{aligned}
t &= \langle \bar{p} | H | \bar{d} \rangle \\
t^d &= \langle d\bar{p} | H | d\bar{d} \rangle \\
t^p &= \langle p\bar{p} | H | p\bar{d} \rangle \\
t^{pd} &= \langle dp\bar{p} | H | dp\bar{d} \rangle
\end{aligned}$$

Within such a formalism the leading perturbative term of the effective exchange integral between the  $i$  and  $j$  vanadium sites comes at the fourth order of perturbation

$$J_{\perp} = -4 \frac{(t^d t^{pd})^2}{(\Delta_1)^2 \Delta_2} - 8 \frac{(t^d t^{pd})^2}{(\Delta_1)^2 U_d} \quad (5)$$

$$= 4J_{1,\perp} + 8J_{2,\perp} \quad (6)$$

where  $\Delta_1 = \delta - U_p + U_d - V_{pd}$  and  $\Delta_2 = 2\delta - U_p + 2U_d - 4V_{pd}$ .

The first term in the expression of  $J_{\perp}$  comes from the configuration  $(|d_i \bar{d}_i p \bar{p}\rangle + |p \bar{p} d_j \bar{d}_j\rangle) / \sqrt{2}$  and while second comes from  $|d_i \bar{d}_i d_j \bar{d}_j\rangle$ . The second term is usually negligible in front of the first one, while that one is equal to  $-4t_{\perp}^2/U_d$ . However, due to the strong contributions of the magnetic electron delocalization on the bridging oxygen, this is not presently true. The ratio between  $J_{1,\perp}$  and  $J_{2,\perp}$  can be evaluated from the singlet wave functions coefficients. Indeed the second order perturbative expression of the singlet wave function is given by

$$\begin{aligned}
|\psi_{Sg}\rangle &= \frac{|d_i p \bar{p} \bar{d}_j\rangle - |\bar{d}_i p \bar{p} d_j\rangle}{\sqrt{2}} + \\
&C_1 \frac{|d_i \bar{d}_i p \bar{d}_j\rangle - |d_i \bar{d}_i \bar{p} d_j\rangle - |d_i \bar{p} d_j p \bar{d}_j\rangle + |\bar{d}_i p d_j p \bar{d}_j\rangle}{2} + \\
&C_2 \frac{|d_i \bar{d}_i p \bar{p}\rangle + p \bar{p} |d_j \bar{d}_j\rangle}{\sqrt{2}} + C'_2 |d_i \bar{d}_i d_j \bar{d}_j\rangle
\end{aligned}$$

where

$$\begin{aligned}
C_1 &= \frac{\sqrt{2} t^{pd}}{\Delta_1} \\
C_2 &= \frac{2 t^p t^{pd}}{\Delta_1 U_d} \\
C'_2 &= \frac{2\sqrt{2} t^d t^{pd}}{\Delta_1 \Delta_2}
\end{aligned}$$

Thus  $(4J_{1,\perp})/(8J_{2,\perp}) = \sqrt{2} C_2 / 2C'_2 \simeq 1.11$  (see Appendix). It comes  $4J_{\perp}^1 \simeq -154.3 \text{ meV}$ .

In the ladder direction the  $O^-$  configurations have negligible weights in the singlet and triplet states, thus the effective exchange integral can be expressed as usual :  $J_{\parallel} = 2K_{\parallel} - 4t_{\parallel}^2/U_d = 2K_{\parallel} + 4J_{1,\parallel}$ , where  $K_{\parallel}$  is the direct exchange integral. The latter is usually considered as negligible, however the extremely small value of  $J_{\parallel}$  imposes to explicitly take these effects into account in the present case. A direct evaluation yields  $K_{\parallel} = 2.0meV$  and the super-exchange contribution comes to be  $4J_{1,\parallel} = 9.1meV$ . One can now properly verify the coherence of our model hopping and exchange parameters :

$$\left(\frac{t_{\perp}}{t_{\parallel}}\right)^2 = 18.7 \quad \simeq \quad \frac{4J_{1,\perp}}{4J_{1,\parallel}} = 17.0$$

From the above analysis it is clear that any method that would not explicitly take into account the delocalization on the bridging oxygen would obtain doubtful evaluations of the effective integrals in the present case. Indeed Smolinski *et al*<sup>24</sup> found hopping integrals in agreement with our results using the LDA+U approach, however their exchange integrals are very different to ours. This discrepancy can be attributed to the fact that they do not take into account the delocalization of the magnetic electron on the bridging oxygen that accounts for half of  $J_{\perp}$  value.

## B. The extended Hubbard Hamiltonian

In addition to the  $t - J$  model, it is possible to obtain from our energy and wave function calculations, the parameters for the extended Hubbard model described in the previous section ; that is a model based on the  $d$  magnetic orbitals of the vanadium atoms and the  $p$  orbitals of the bridging oxygen in the rung geometry. The parameter extraction will be done using a least square fit method where both the energy differences and the wave functions coefficients of the extended Hubbard model are fitted on the computed *ab initio* wave functions and energies, according to the intermediate Hamiltonian theory<sup>25</sup>. The different parameters of the Hubbard Hamiltonian are therefore optimized so that the Hubbard secular equations of the singlet, triplet and the two doublets are verified with the computed wave functions (taken as the normalized projection onto the CAS of the *DDCI2* wave functions) and the computed energy differences. The resulting parameters in the rung geometry are summarized in table II.

These values are in reasonable agreement with the vanadium on site

repulsion obtained from the ladder geometry

$$U_d = 4 (t_{\parallel})^2 / (2K_{\parallel} - J_{\parallel}) = 6.8eV$$

## V. CONCLUSION

We computed the effective hopping and exchange integrals of a  $t - J$  Hamiltonian for the high temperature phase of  $\alpha'NaV_2O_5$ . The parameters evaluations were performed using an embedded cluster approach devised to properly take into account the electrostatic and exclusion effects of the rest of the crystal as well as dynamical polarization and correlation effects within the cluster. The results yield dominant interactions to be the delocalization of the magnetic electrons on the ladder rungs. This incredibly large delocalization is mediated by the appropriate  $p$  orbital of the bridging oxygen. In fact the magnetic electrons should not be seen as supported by the  $d$  orbitals of the vanadium atoms in a quarter-filled system, but by orbitals delocalized on the 3 atoms of the rungs, that is on the  $d$  orbitals of the two vanadium atoms and the  $p$  orbital of the bridging oxygen. In such a representation the system is no longer quarter-filled but half-filled. The remaining interactions between these delocalized magnetic electrons devise a two-dimensional triangular Heisenberg system where the effective exchange in the ladder direction is anti-ferromagnetic while it is ferromagnetic in the two other directions.

In addition to the  $t - J$  parameters evaluation, a thorough analysis of the *ab-initio* variational wave functions allowed us to evaluate the relative amplitudes of the underlying three-bands extended Hubbard Hamiltonian. The negligible difference obtained between the oxygen on-site repulsion and the  $p-d$  orbital energy difference,  $U_p - \delta < 0.03eV$ , yields a quasi-degeneracy between the configurations where the magnetic electron is located on one of the  $d$  orbitals of the vanadium atoms and the  $p$  orbital of the bridging oxygen. It results in the delocalization of the magnetic electrons on the rungs.

## ACKNOWLEDGMENTS

We thank Jean-Pierre Daudey, Jean-Paul Malrieu, Frédéric Mila and Timothy Ziman for many fruitful discussions, T. Chatterji for crystallographic data, Thierry Leininger and Daniel Maynau for computational help and development. The CASCSF calculations were done using

the MOLCAS package<sup>26</sup>, the DDCI calculations were done using the CASDI package written by Daniel Maynau and Nadia Ben Amor<sup>27</sup>. Part of the calculations were performed at IDRIS/CNRS under project number 1104.

## APPENDIX

The wave functions obtained at the DDCI2 level are developed onto wave functions including up to 592000 Slater determinants (according to the state and the geometry), nevertheless their major contributions are within the CAS space. The CAS configurations of the computed wave functions are reported below, after relocalization of the optimized CAS orbitals. This was done by the mean of a procedure based on Boys' method<sup>28</sup>.

In the rung geometry

$$\begin{aligned}
|\phi_{Sg}\rangle &= 0.84 \frac{|d_i p \bar{p} \bar{d}_j\rangle - |\bar{d}_i p \bar{p} d_j\rangle}{\sqrt{2}} + \\
& 0.47 \frac{|d_i \bar{d}_i p \bar{d}_j\rangle - |d_i \bar{d}_i \bar{p} d_j\rangle - |d_i \bar{p} d_j \bar{d}_j\rangle + |\bar{d}_i p d_j \bar{d}_j\rangle}{2} + \\
& 0.14 \frac{|d_i \bar{d}_i p \bar{p}\rangle + |p \bar{p} d_j \bar{d}_j\rangle}{\sqrt{2}} + 0.09 |d_i \bar{d}_i d_j \bar{d}_j\rangle \\
& + \text{small terms} \dots
\end{aligned}$$

$$\begin{aligned}
|\phi_{Tp}\rangle &= 0.90 \frac{|d_i p \bar{p} \bar{d}_j\rangle + |\bar{d}_i p \bar{p} d_j\rangle}{\sqrt{2}} + \\
& 0.38 \frac{|d_i \bar{d}_i p \bar{d}_j\rangle + |d_i \bar{d}_i \bar{p} d_j\rangle - |d_i \bar{p} d_j \bar{d}_j\rangle - |\bar{d}_i p d_j \bar{d}_j\rangle}{2} \\
& + \text{small terms} \dots
\end{aligned}$$

$$\begin{aligned}
|\phi_{D_+}\rangle &= 0.62 \frac{|d_i p \bar{p}\rangle + |p \bar{p} d_j\rangle}{\sqrt{2}} + \\
& 0.69 \frac{-2|d_i \bar{p} d_j\rangle + |\bar{d}_i p d_j\rangle + |d_i p \bar{d}_j\rangle}{\sqrt{6}} + \\
& 0.12 \frac{|d_i \bar{d}_i d_j\rangle + |d_i d_j \bar{d}_j\rangle}{\sqrt{2}} + \\
& 0.12 \frac{|d_i \bar{d}_i p\rangle - |p d_j \bar{d}_j\rangle}{\sqrt{2}} \\
& + \text{small terms} \dots
\end{aligned}$$

$$\begin{aligned}
|\phi_{D_-}\rangle &= 0.65 \frac{|d_i p \bar{p}\rangle - |p \bar{p} d_j\rangle}{\sqrt{2}} - \\
& 0.65 \frac{|\bar{d}_i p d_j\rangle - |d_i p \bar{d}_j\rangle}{\sqrt{2}} - \\
& 0.06 \frac{|d_i \bar{d}_i d_j\rangle - |d_i d_j \bar{d}_j\rangle}{\sqrt{2}} + \\
& 0.11 \frac{|d_i \bar{d}_i p\rangle + |p d_j \bar{d}_j\rangle}{\sqrt{2}} \\
& + \text{small terms} \dots
\end{aligned}$$

In the ladder geometry

$$|\phi_{Sg}\rangle = 0.92 \frac{|d_i p_x \bar{p}_x p_y \bar{p}_y \bar{d}_j\rangle - |\bar{d}_i p_x \bar{p}_x p_y \bar{p}_y d_j\rangle}{\sqrt{2}} + \text{small terms} \dots$$

$$|\phi_{Tp}\rangle = 0.92 \frac{|d_i p_x \bar{p}_x p_y \bar{p}_y \bar{d}_j\rangle + |\bar{d}_i p_x \bar{p}_x p_y \bar{p}_y d_j\rangle}{\sqrt{2}} + \text{small terms} \dots$$

$$\begin{aligned}
|\phi_{D_+}\rangle &= -0.78 \frac{|d_i p_x \bar{p}_x p_y \bar{p}_y\rangle + |p_x \bar{p}_x p_y \bar{p}_y d_j\rangle}{\sqrt{2}} \\
& + 0.46 \frac{-2|d_i \bar{p}_x p_y \bar{p}_y d_j\rangle + |\bar{d}_i p_x p_y \bar{p}_y d_j\rangle + |d_i p_x p_y \bar{p}_y \bar{d}_j\rangle}{\sqrt{6}} \\
& - 0.15 \frac{|\bar{d}_i p_x \bar{p}_x p_y d_j\rangle - |d_i p_x \bar{p}_x p_y \bar{d}_j\rangle}{\sqrt{2}} \\
& + 0.07 \frac{|d_i \bar{d}_i p_x p_y \bar{p}_y\rangle - |p_x p_y \bar{p}_y d_j \bar{d}_j\rangle}{\sqrt{2}} \\
& - 0.04 \frac{|d_i \bar{d}_i p_x \bar{p}_x p_y\rangle - |p_x \bar{p}_x p_y d_j \bar{d}_j\rangle}{\sqrt{2}} \\
& + \text{small terms} \dots
\end{aligned}$$

$$\begin{aligned}
|\phi_{D_-}\rangle &= +0.82 \frac{|d_i p_x \bar{p}_x p_y \bar{p}_y\rangle - |p_x \bar{p}_x p_y \bar{p}_y d_j\rangle}{\sqrt{2}} \\
& - 0.31 \frac{|\bar{d}_i p_x p_y \bar{p}_y d_j\rangle - |d_i p_x p_y \bar{p}_y \bar{d}_j\rangle}{\sqrt{2}} \\
& - 0.28 \frac{-2|d_i p_x \bar{p}_x \bar{p}_y d_j\rangle + |\bar{d}_i p_x \bar{p}_x p_y d_j\rangle + |d_i p_x \bar{p}_x p_y \bar{d}_j\rangle}{\sqrt{6}} \\
& - 0.08 \frac{|d_i \bar{d}_i p_x p_y \bar{p}_y d_j\rangle + |d_i p_x p_y \bar{p}_y d_j \bar{d}_j\rangle}{\sqrt{2}}
\end{aligned}$$

$$+0.04 \frac{|d_i \bar{d}_i p_x \bar{p}_x p_y\rangle - |p_x \bar{p}_x p_y d_j \bar{d}_j\rangle}{\sqrt{2}}$$

+small terms ...

- <sup>1</sup> J. W. Bray, H. R. Hart Jr., L. V. Interrante, I. S. Kasper, G. D. Watkins, S. H. Wee and J. C. Bonner, *Phys. Rev Lett.* **35**, 744 (1975); D. E. Moncton, R. J. Birgeneau, L. V. Interrante and F. Wudl, *Phys. Rev Lett.* **39**, 507 (1977); S. Huizinga, J. Kommandeur, G. A. Sawatzky, B. T. Thole, K. Kopinga, W. J. M de Jonge and J. Roos, *Phys. Rev B* **19**, 4723 (1979).
- <sup>2</sup> M. Hase, I. Terasaki and K. Uchinokura, *Phys. Rev Lett.* **70**, 3651 (1993).
- <sup>3</sup> A. Hardy, J. Galy, A. Casalot, M. Pouchard, *Bull. Soc. Chem. Fr.* **4**, 1056 (1965).
- <sup>4</sup> M. Isobe and Y. Ueda, *J. Phys. Soc. Jnp.* **65**, 1178 (1996); M. Weiden, R. Hauptmann, C. Geidel, F. Steglich, M. Fischer, P. Lemmens and G. Güntherodt, *Z. Phys. B* **103**, 1 (1997); Y. Fujii, H. Nakao, T. Yosihama, M. Nishi, K. Nakajima, K. Kakurai, M. Isobe, Y. Ueda and H. Sawa, *J. Phys. Soc. Jnp* **66**, 326 (1997).
- <sup>5</sup> T. Yoshihama, M. Nishi, K. Nakajima, K. Kakurai, Y. Fujii, M. Isobe, C. Kagami and Y. Ueda, *J. Phys. Soc. Jpn.* **67**, 744 (1998).
- <sup>6</sup> W. Schnelle, U. Grin and R. K. Kremer, *Phys. Rev.* **B59**, 73 (1999).
- <sup>7</sup> L. N. Bulaevskii, A. I. Buzdin and D. I. Khomskii, *Solid State Commun.* **27**, 5 (1978).
- <sup>8</sup> A. N. Vasil'ev, V. V. Pryadun, D. I. Khomskii, G. Dhalenne, A. Revcolevschi, M. Isobe and Y. Ueda, *Phys. Rev. Letters* **81**, 1949 (1998).
- <sup>9</sup> J. Galy, A. Casalot, M. Pouchard and P. Hagenmuller, *Séance C. R. Acad. Sc. Paris C* **262**, 1055 (1966); A. Carpy and J. Galy, *Acta Cryst.* **B 31**, 1481 (1975).
- <sup>10</sup> H. G. Von Schnering, Y. Grin, M. Kaupp, M. Somer R. K. Kremer, O. Jepsen, T. Chatterji and M. Weiden, *Z. Kristallogr.* **213**, 246 (1998); T. Chatterji, K. D. Liß, G. J. McIntyre, M. Weiden, R. Hauptmann and C. Geibel, *Solid Stat. Comm.* **108**, 23 (1998); A. Meetsma, J. L. de Boer, A. Damascelli, T. T. M. Palstra, J. Jegoudez and A. Revcolevschi, *Acta. Cryst.* **C 54**, 1558 (1998).
- <sup>11</sup> J. Galy, *J. Solid State Chem.* **100**, 229 (1992).
- <sup>12</sup> W.S. Bacsá, R. Lewandowska, A. Zwick, *preprint*.
- <sup>13</sup> N. W. Winter, R. M. Pitzer and D. K. Temple, *J. Chem. Phys.* **86**, 3549 (1987).
- <sup>14</sup> P. Durand *et al*, *Theor. Chim. Acta* **38**, 283 (1975).
- <sup>15</sup> P.E.M. Siegbahn, J. Almlöf, A. Heiberg and B.O. Roos, *J. Chem. Phys.* **74**, 2384 (1981).
- <sup>16</sup> V. M. García, O. Castell, R. Caballol and J.P. Malrieu, *Chem. Phys. Lett* **238**, 222 (1995); V. M. García, M. Reguero and R. Caballol, *Theor. Chem. Acc.* **98**, 50 (1997).
- <sup>17</sup> J. P. Malrieu, *J. Chem. Phys.* **47**, 4555 (1967); P. de Loth, P. Cassoux, J. P. Daudey and J. P. Malrieu, *J. Am. Chem. Soc.* **103**, 4007 (1981); M. F. Charlot, M. Verdaguer, Y. Journaux, P. de Loth and J. P. Daudey, *Inorg. Chem.* **23**, 3802 (1984); R. Broer and W.J.A. Maaskant, *Chem. Phys.* **102**, 103 (1986); J. Miralles, J. P. Daudey and R. Caballol, *Chem. Phys. Lett.* **198**, 555 (1992); J. Miralles, O. Castell, R. Caballol and J. P. Malrieu, *Chem. Phys.* **172**, 33 (1993); K. Handrick, J. P. Malrieu and O. Castell, *J. Chem. Phys.* **101**, 2205 (1994).
- <sup>18</sup> C. J. Calzado, J. F. Sanz, J.P. Malrieu and F. Illas, *Chem. Phys. Letters* **307**, 102 (1999).
- <sup>19</sup> C. de Graaf, I. de P.R. Moreira, F. Illas and R. L. Martin, *Phys. Rev.* **B 60**, 3457 (1999).
- <sup>20</sup> Z. Barandiarán and L. Seijo, *Can. J. Chem.* **70**, 409 (1992).
- <sup>21</sup> V.R. Saunders, R. Dovesi, C. Roetti, M. Causà, N.M. Harrison, R. Orlando, C.M. Zicovich-Wilson, **CRYSTAL98 User's Manual**, University of Torino, Torino, (1998).
- <sup>22</sup> Vanadium : W.C. Mackrodt, N.M. Harrison, V.R. Saunders, N.L. Allan, M.D.Towler,

- E. Apra and R. Dovesi, *Philos. mag.* **A 68**, 653 (1993);  
 Sodium : M. Prencipe, A. Zupan, R. Dovesi, E. Apra and V. R. Saunders, *Phys. Rev* **B 51**, 3391 (1995);  
 Oxygen : E. Apra, M. Causa, M. Prencipe, R. Dovesi and V.R. Saunders, *J. Phys. Condens. Matter* **5**, 2969 (1993).
- <sup>23</sup> P. Horsch and F. Mack, *Eur. Phys. J.* **B 5**, 367 (1998).
- <sup>24</sup> H. Smolinski, C. Gros, W. Weber, U. Peuchert, G. Roth, M. Weiden and C. Geidel, *Phys. Rev. Lett.* **80**, 5164 (1998)  $t_{\parallel} = -562meV$ ,  $t_{\perp} = -185meV$ ,  $t' = +12meV$ ,  $J_{\parallel} = -65meV$ ,  $J_{\perp} = -77meV$
- <sup>25</sup> J.P. Malrieu, Ph. Durand and J.P. Daudey, *J. Phys. A: Math. Gen.* **18**, 809 (1985);  
 For a review on effective Hamiltonians see: Ph. Durand and J.P. Malrieu in *Ab-initio methods in quantum chemistry*, ed. K.P. Lawley, John Wiley p. 321 (1987).
- <sup>26</sup> MOLCAS suite of programs.  
 K. Anderson, M. P. Fülscher, G. Karlström, R. Lindh, P. A. Malqvist, J. Olsen, B. Roos, A. J. Sadlej, M. R. A. Blomberg, P. E. M. Siegbahn, V. Kello, J. Noga, M. Urban, P. O. Widmark, MOLCAS Version 4, Dpt of Theor. Chem., Chem. Center, Univ. of LUND, P. O. B. 124, S-221 00 Lund, Sweden, Lund 1994.
- <sup>27</sup> CASDI suite of programs.  
 N. Ben Amor and D. Maynau, *Chem. Phys. Letters* **286**, 211 (1998).
- <sup>28</sup> S. F. Boys, *R. Mod. Phys.* **32**, 296 (1960); J.M. Foster, S. F. Boys, *R. Mod. Phys.* **32**, 300 (1960).

TABLE I. Exchange and hopping parameters in  $meV$  for a  $t - J$  Hamiltonian computed at different levels of calculation.

Calculation level	CASCI	IDDCI1	DDCI2
Physics included	Valence shell	+dynamical polarization	+dynamical polarization and correlation
$J'$	+5.48	+4.14	+4.87
$t'$	+37.5	+28.7	+44.2
$J_{\parallel}$	-1.05	-4.64	-5.04
$t_{\parallel}$	-115.8	-176.5	-124.6
$J_{\perp}$	-60.6	-321.1	-293.5
$t_{\perp}$	-420.6	-542.7	-538.2

TABLE II. Parameters in eV of the extended Hubbard Hamiltonian in the rung geometry.

$t_{\perp}^p$	$t_{\perp}^d$	$t_{\perp}^{pd}$	$U_d - V_{pd}$	$U_p - \delta$
1.1	2.0	1.3	3.6	< .03

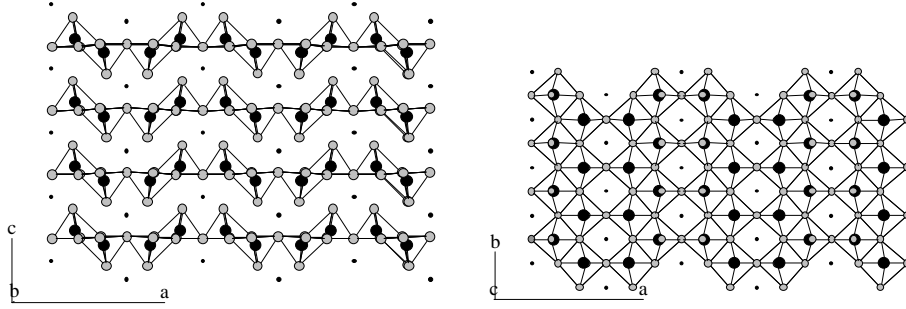


FIG. 1. Schematic structure of  $\alpha'$   $\text{NaV}_2\text{O}_5$ , a) along the a-c plane, b) along the a-b plane. The oxygen atoms are denoted by open circles, the vanadium atoms by filled circles and the sodium atoms by dots.

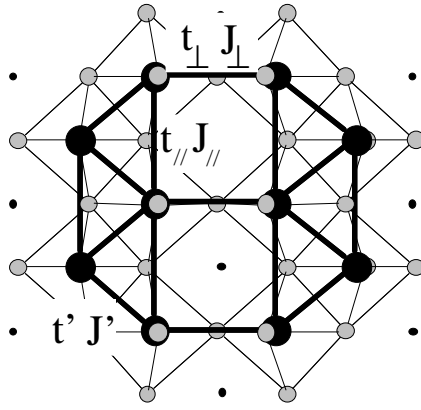


FIG. 2. The three different types of NN interactions:  $t_{\parallel}$  and  $J_{\parallel}$ ,  $t_{\perp}$  and  $J_{\perp}$ ,  $t'$  and  $J'$ .

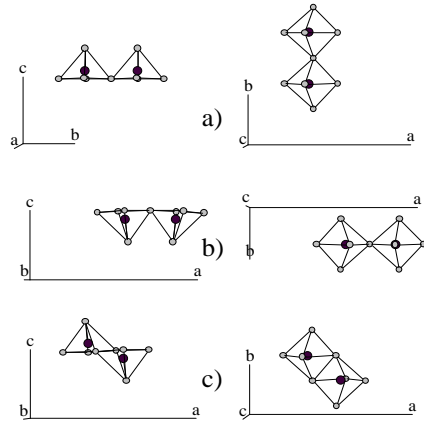


FIG. 3. Fragments of the crystal used for the cluster calculations. a)  $t_{\parallel}$ , and  $J_{\parallel}$  ; b)  $t_{\perp}$ , and  $J_{\perp}$  ; c)  $t'$ , and  $J'$ .

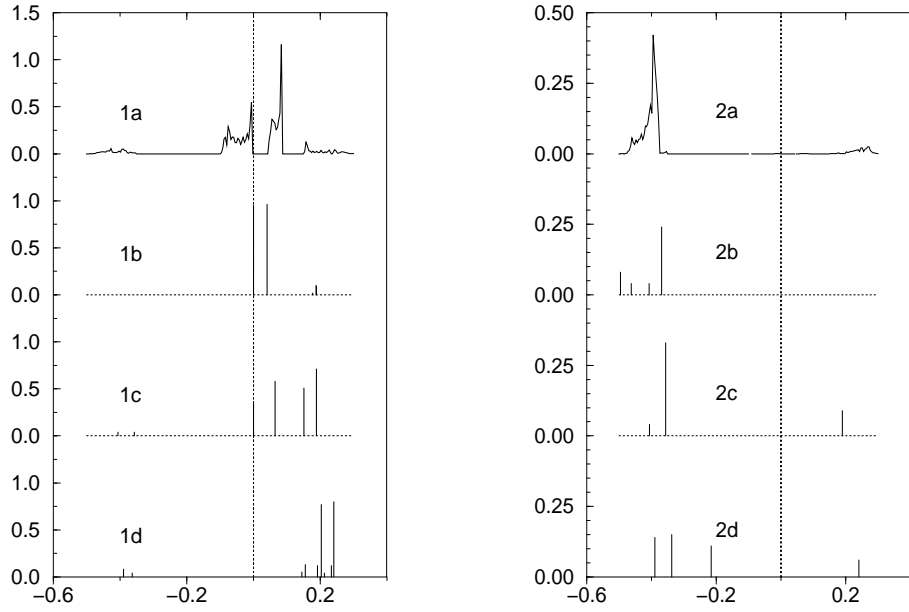


FIG. 4. Projected DOSS on the  $d$  magnetic atomic orbitals (1) and the  $p$  orbital of the bridging oxygen atom in the rung geometry (2). The crystal HF calculation (a). The rung cluster of this work (b). The rung cluster embedded with only one type of oxygen atom, all atoms supporting their formal charges (c). The rung cluster without embedding (d). The dotted vertical line shows the Fermi level.

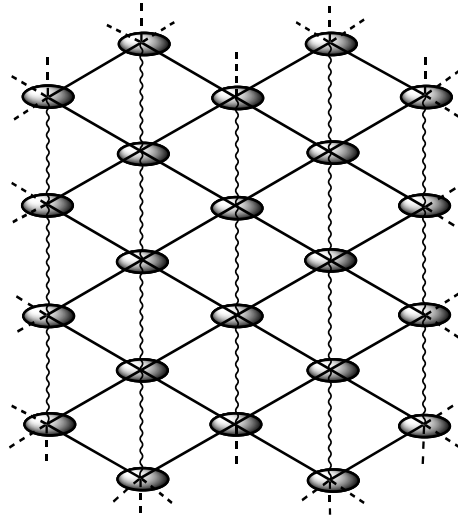


FIG. 5. Equivalent magnetic system. The ellipsoids represent the delocalized magnetic electron on the rungs. The straight lines represent the ferromagnetic remaining interactions ( $J'_{eff}$ ) while the zig-zag lines represent the anti-ferromagnetic ones ( $J_{\parallel}^{eff}$ ).